Spinup Maneuver and Nonlinear Active Nutation Damping

Hwa-Suk Oh*
Electronics and Telecommunications Research Institute, Taejon 305-606, Republic of Korea

Introduction

WHEEL spinup maneuvering strategies are still being studied and used in spin axis turn or flat spin recovery.[1,2] There remains some residual transverse angular momentum in the spacecraft body causing nutation at the end of the spinup maneuver. The predetermined or optimal variable wheel speed method[3,4] was suggested to reduce the residual nutation. The nutation is damped out when the angular velocity vector is aligned with the system momentum vector. Stabilization to an equilibrium point depends on the number of available actuators.[5–8]

A bias momentum satellite can use its wheel as an active damping actuator.[9,10] A bias momentum wheel is one of the candidate stabilizing devices for the Electronics and Telecommunications Research Institute's proposed experimental communications satellite (ETRI ECS-1). The objective of this Note is to study the design feasibility of a nonlinear feedback control law of a single momentum wheel for suppressing the satellite wobbling induced by spinup while sustaining the wheel momentum near a nominal value.

Dynamic Characteristics

The system dynamic equations can be written as

$$\boldsymbol{I}\dot{\boldsymbol{\omega}} = -\boldsymbol{\omega}^{\times}\boldsymbol{I}\boldsymbol{\omega} - \boldsymbol{\omega}^{\times}h_w\boldsymbol{l}_3 - u\boldsymbol{l}_3 \tag{1a}$$

$$\dot{h}_w = u \tag{1b}$$

where $\boldsymbol{I}$ is the system inertia matrix, h_w the wheel relative angular momentum, $\boldsymbol{l}_3 \equiv [0\ 0\ 1]^T$, and $\boldsymbol{\omega}^{\times}$ the cross product matrix of the angular velocity vector $\boldsymbol{\omega}$. Products of inertia I_{12} and I_{13} are negligible, and thus the system equations are simplified as

$$I_{11}\dot{\omega}_1 = (I_{22} - I_{33})\omega_2\omega_3 + I_{23}\left(\omega_3^2 - \omega_2^2\right) - h_w\omega_2 \tag{2a}$$

$$I_{22}\dot{\omega}_2 + I_{23}\dot{\omega}_3 = (I_{33} - I_{11})\omega_1\omega_3 + I_{23}\omega_1\omega_2 + h_w\omega_1 \tag{2b}$$

$$I_{23}\dot{\omega}_2 + I_{33}\dot{\omega}_3 = (I_{11} - I_{22})\omega_1\omega_2 - I_{23}\omega_1\omega_3 - u \tag{2c}$$

For fast Earth acquisition after the spinup maneuver, the body must rotate at nonzero velocity. The final desired angular velocity is thus assumed nonzero here. The nonzero equilibrium points are constrained by $\boldsymbol{I}\boldsymbol{\omega} + h_w\boldsymbol{l}_3 = \lambda\boldsymbol{\omega}$, where λ denotes an equilibrium constant.[11] Given a nominal wheel momentum $h_w = h_n$ at an equilibrium, then the angular velocity vector satisfies

$$\begin{bmatrix}\omega_1\\ \omega_2\\ \omega_3\end{bmatrix} = \begin{bmatrix}\nu_1\\ \dfrac{I_{23}h_n}{(I_{33}-\lambda)(I_{22}-\lambda) - I_{23}^2}\\ \dfrac{-(I_{22}-\lambda)h_n}{(I_{33}-\lambda)(I_{22}-\lambda) - I_{23}^2}\end{bmatrix} \tag{3}$$

where ν_1 is a constant. It is clear from Eq. (3) that when the product of inertia is nonzero, the momentum wheel axis cannot be aligned with the angular momentum vector at the equilibrium state.

Received Dec. 13, 1994; revision received Oct. 17, 1995; accepted for publication Oct. 23, 1995.

*Senior Researcher, Satellite Communications Division, P.O. Box 106, Yusong. Member AIAA.

Spinup Conditions

At the end of the spinup maneuver, the spacecraft angular velocity oscillates around the nonzero angular velocity equilibrium points $\boldsymbol{\omega}_e$ that satisfy the equilibrium condition Eq. (3). Among those equilibrium points, first consider the case when $\omega_{1e} = \nu_1 \neq 0$. The equilibrium values of ω_{2e} and ω_{3e} have uniquely fixed values because $\lambda \equiv I_{11}$ when $\nu_1 \neq 0$. From the conservation principle of the system angular momentum, the final system angular momentum H_f remains identical to the initial angular momentum H_0 as $H_0 = H_f = \lambda\|\boldsymbol{\omega}_e\|$, and thus H_0 satisfies the inequality

$$H_0 > I_{11}\sqrt{\omega_{2e}^2 + \omega_{3e}^2} \tag{4}$$

This is a necessary condition for $\nu_1 \neq 0$.

Conversely, if the initial system angular momentum is small enough such that

$$H_0 \leq I_{11}\sqrt{\omega_{2e}^2 + \omega_{3e}^2} = \frac{I_{11}h_n\sqrt{I_{23}^2 + (I_{22} - I_{11})^2}}{(I_{33} - I_{11})(I_{22} - I_{11}) - I_{23}^2} \tag{5}$$

then ω_{1e} should become zero. In other words, by starting the spinup maneuver with a small initial system angular momentum satisfying Eq. (5), the angular velocity ω_1 oscillates around zero at the end of maneuver, i.e., Eq. (5) is a sufficient condition for $\omega_{1e} \equiv 0$ at the end of spinup. When the product of inertia $I_{23} \equiv 0$, then Eq. (5) turns into the sufficient condition for the spin axis convergence shown in Ref. 1. Without loss of generality, we let $\omega_{1e} \equiv 0$ be the desired equilibrium point for spinup maneuver in this study.

Active Damping Design

The control objective is to suppress the oscillating angular velocity to the constant value ω_e while keeping the wheel momentum near the nominal value. Among several nonlinear control design techniques, a feedback linearization approach is considered in this study. Unfortunately, the system is neither locally controllable nor involutive. Therefore, rather than trying to find an output function of relative degree four, let us try to find an output function y of lower relative degree, e.g., two, for simple derivation.

First, consider a system with a general inertia matrix. To simplify the control law expression, Eq. (1a) is converted to

$$\dot{\boldsymbol{h}} = \boldsymbol{h}^{\times}\boldsymbol{J}\boldsymbol{h} + h_w\boldsymbol{l}_3^{\times}\boldsymbol{J}\boldsymbol{h} - u\boldsymbol{l}_3 \tag{6}$$

where new state variables are defined as $\boldsymbol{h} \equiv \boldsymbol{I}\boldsymbol{\omega}$ and $\boldsymbol{J} \equiv \boldsymbol{I}^{-1}$. Consider an output function $y = y(\boldsymbol{h})$, i.e., a function of angular momentum $\boldsymbol{h}$ only. Necessary conditions[12] for relative degree two lead to

$$L_g y = 0 \tag{7a}$$

$$L_g L_f y + \frac{\partial(L_f y)}{\partial h_w} \neq 0 \qquad \text{at} \qquad \boldsymbol{h} \equiv 0 \tag{7b}$$

where the Lie derivative $L_{\boldsymbol{f}}$, $\boldsymbol{f}$, and $\boldsymbol{g}$ are defined as

$$L_g y \equiv \left[\frac{\partial y}{\partial \boldsymbol{h}}\right]\boldsymbol{g} \tag{8a}$$

$$\boldsymbol{f} \equiv \boldsymbol{h}^{\times}\boldsymbol{J}\boldsymbol{h} + h_w\boldsymbol{l}_3^{\times}\boldsymbol{J}\boldsymbol{h} \tag{8b}$$

$$\boldsymbol{g} \equiv -\boldsymbol{l}_3 \tag{8c}$$

From Eqs. (7a) and (7b), necessary conditions for y result in

$$\frac{\partial y}{\partial h_3} = 0 \tag{9a}$$

$$\frac{\partial y}{\partial h_1}(\boldsymbol{0})J_{23} - \frac{\partial y}{\partial h_2}(\boldsymbol{0})J_{13} \neq 0 \tag{9b}$$

Since $J_{13} = 0$, y needs to include at least one linear term of h_1. We can see in Eq. (2a) that the desired state $\omega_{1e} \equiv 0$ (i.e., $h_1 \equiv 0$) leads both h_2 and h_3 to constant values, i.e., an equilibrium point. Therefore, suppressing ω_1 to zero makes the system converge to one

of the candidate objective equilibrium points, and the selection of output function $y \equiv h_1$ is reasonable.

Following the systematic procedure for the feedback linearization,[12] the system equations are transformed to (with definition $z_1 \equiv y \equiv h_1$)

$$\dot{z}_1 = z_2 \tag{10a}$$

$$\dot{z}_2 = L_f^2 y + \left[L_g L_f y + \frac{\partial (L_f y)}{\partial h_w} \right] u \tag{10b}$$

A candidate control law can then be chosen as

$$u = \left[L_g L_f y + \frac{\partial (L_f y)}{\partial h_w} \right]^{-1} \left[-L_f^2 y - k_1 z_1 - k_2 z_2 \right] \tag{11}$$

Momentum Management

The control law just chosen stabilizes the system to an equilibrium point such as $\omega_1 \equiv 0$, and ω_2, ω_3, and h_w are all constants. The requirement of h_w is to keep the wheel momentum near the nominal value at the end of damping while sustaining it within a user-specified design limit during the damping maneuver. This can be satisfied by just adding an on–off control logic on the $\dot{h}_w$ control law in Eq. (11). Suppose that the wheel momentum deviation from the nominal value is restricted within h_{lim}. Then the control law $\dot{h}_w$ is turned on only if either of the following conditions is satisfied:

$$|h_w - h_n| < h_{\text{lim}} \tag{12a}$$

$$\text{sgn}[(h_w - h_n)\dot{h}_w] \leq 0 \tag{12b}$$

In addition, h_{lim} is to be decreased exponentially as follows to make h_w converge to the nominal value:

$$h_{\text{lim}} = h_{\text{lim}}(t_0) \exp\left[-\frac{(t - t_0)}{T} \right] \tag{13}$$

where $h_{\text{lim}}(t_0)$ is the design limit of the momentum deviation and T is the momentum convergence time constant. If the time constant is small, it degrades the nutation damping performance; conversely, if the time constant is large, it degrades the momentum convergence performance. It is not hard to find a proper time constant. Even though we cannot expect a control law to directly stabilize both the wheel momentum and the angular velocity, the wheel momentum is regulated to the nominal value indirectly by applying the switching logic of Eqs. (12) and (13).

Simulations

ETRI ECS-1 is to be equipped with a bias momentum wheel with $h_n = 55$ kg-m^2/s. The system inertia terms are given as $I_{11} = 500$, $I_{22} = 400$, $I_{33} = 440$, $I_{23} = -7$, and $I_{12} = I_{13} = 0$ kg-m^2. After injection to a drift orbit, the spacecraft body is rotating at about 5 rpm around the first body axis with the wheel speed zero. By spinning up the momentum wheel to the nominal value h_n, a part of the body momentum is transferred to the wheel, and the angular velocity vector oscillates around the final desired equilibrium point. Since the initial system angular momentum H_0 is sufficiently low, the equilibrium angular velocity ω_{1e} becomes zero at the end of the spinup maneuver as expected.

With the initial state $\omega = [1.20 \ -1.16 \ 26.85]^T$ deg/s at an arbitrary time after the spinup maneuver, the feedback gains $k_1 = k_2 = 0.015$, and the time constant $T = 100$ s, simulation shows good damping performance. The wheel momentum is sustained within 10% of the nominal value during damping and converges to the nominal value as shown in Fig. 1. The system momentum vector also converges to its desired equilibrium position, as shown in Fig. 2. The convergence to the desired equilibrium was found insensitive to the initial state with the given time constant.

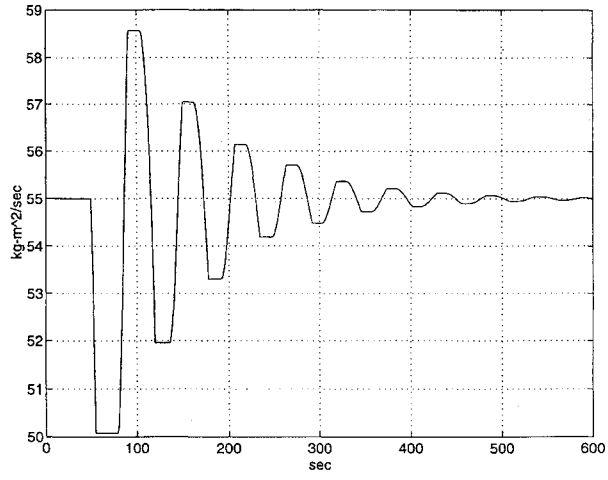

Fig. 1 Wheel angular momentum control.

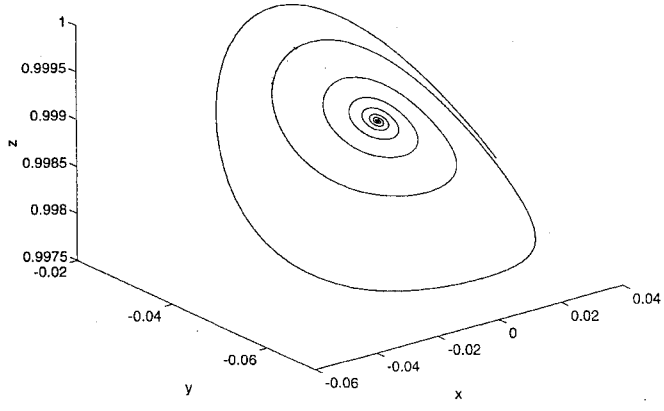

Fig. 2 Normalized system angular momentum.

Conclusions

A sufficient condition of the initial system momentum magnitude H_0 for the convergence to a desired equilibrium at the spinup maneuver has been derived. A nonlinear nutation damping control law has been designed for a proposed ECS. Simulation results show that the nutation has been successfully suppressed by making the angular velocity converge to the system angular momentum while the wheel momentum is kept near the nominal value at the end of damping. The peak wheel momentum is also kept within the design limit satisfactorily.

References

[1]Barba, P. M., and Aubrun, J. N., "Satellite Attitude Acquisition by Momentum Transfer,"*AIAA Journal*, Vol. 14, No. 10, 1976, pp. 1382–1386.

[2]Hall, C. D., and Rand, R. H., "Spinup Dynamics of Axial Dual-Spin Spacecraft," *Journal of Guidance, Control, and Dynamics*, Vol. 17, No. 1, 1994, pp. 30–37.

[3]Vigneron, F. R., and Staley, D. A., "Satellite Attitude Acquisition by Momentum Transfer—The Controlled Wheel Speed Method," *Celestial Mechanics*, Vol. 27, No. 1, 1982, pp. 111–130.

[4]Vadali, S. R., and Junkins, J. L., "Spacecraft Large Angle Rotational Maneuvers with Optimal Momentum Transfer," *Journal of the Astronautical Sciences*, Vol. 31, No. 2, 1983, pp. 217–235.

[5]Byrnes, C. I., and Isidori, A., "On the Attitude Stabilization of Rigid Spacecraft," *Automatica*, Vol. 27, No. 1, 1991, pp. 87–95.

[6]Krishnan, H., Reyhanoglu, M., and McClamroch, H., "Attitude Stability of a Rigid Spacecraft Using Two Control Torques: A Nonlinear Control Approach Based on Spacecraft Attitude Dynamics," *Automatica*, Vol. 30, No. 6, 1994, pp. 1023–1027.

[7]Aeyels, D., and Szafranski, M., "Comments on the Stabilizability of the Angular Velocity of a Rigid Body," *Systems and Control Letters*, Vol. 10, No. 1, 1988, pp. 35–39.

[8]Guelman, M., "On Gyrostat Dynamics and Recovery," *Journal of the Astronautical Sciences*, Vol. 37, No. 2, 1989, pp. 109–119.

[9]Phillips, K., "Active Nutation Damping Utilizing Spacecraft Mass Properties," *IEEE Transactions on Aerospace and Electronic Systems*, Vol. AES-9, No. 5, 1973, pp. 688–693.

[10]Smay, J. W., and Slafer, L. I., "Dual-Spin Spacecraft Stabilization Using Nutation Feedback and Inertia Coupling," *Journal of Spacecraft and Rockets*, Vol. 13, No. 11, 1976, pp. 650–659.
[11]Hughes, P. C., *Spacecraft Attitude Dynamics*, Wiley, New York, 1986, Chap. 6.
[12]Slotine, J.-J. E., and Li, W., *Applied Nonlinear Control*, Prentice–Hall, Englewood Cliffs, NJ, 1991, Chap. 6.

Scanning Horizon Sensor Attitude Correction for Earth Oblateness

Jonathan A. Tekawy,* Patrick Wang,† and Charles W. Gray‡
The Aerospace Corporation, El Segundo, California 90245-4691

Introduction

EARTH-ORIENTED satellites typically use horizon sensors to estimate and correct their roll and pitch errors with respect to the local vertical. A low Earth orbit (LEO) satellite can achieve roll and pitch attitude determination accuracy on the order of 0.1 deg using a single scanning horizon sensor. However, the sensor accuracy is limited by errors arising from various sources.[1] From these various sources, the Earth oblateness contributes significant effects on the sensor measurement errors, which propagate directly to the satellite attitude estimates. Several authors (e.g., Ref. 1 and the references therein) have studied the horizon sensors and impact of oblate Earth on the attitude errors. Most of the results, however, have been limited in scope and scattered in the open literature and internal technical documents. In the Note, we will show a complete and simple method to determine and correct roll and pitch errors caused by Earth oblateness for single and scanning type horizon sensor configurations.

Horizon Sensor Roll/Pitch Attitude Determination

Figure 1 shows how the horizon scanner operates for a spinning sensor. As the sensor scans the space, its field of view (FOV) crosses the Earth horizon periodically and defines the horizon crossing vectors. Assuming a spherical Earth, the incoming and outgoing horizon crossing vectors in the satellite body frame (i.e., $\boldsymbol{L}_i^B$ and $\boldsymbol{L}_o^B$) can be defined as a function of the half-cone angle α, canting angle γ, and crossing angles β_i and β_o, as well the crossing vectors in the sensor frame. For notation simplicity, the canting angle is assumed to rotate about the satellite Y^B axis. The sensor frames at both space-to-Earth and Earth-to-space crossing locations can be defined as follows: 1) Z axis coincides with the Earth crossing vectors, 2) Y axis is normal to the plane defined by the sensor cone axis and Earth crossing vectors, and 3) to complete the triad, X axis has to satisfy the right-hand rule. Using Fig. 1, Euler rotations can be obtained to transform these specific sensor frames to the satellite body frame. Thus, the unit vectors in degree at the Earth and space crossing in the satellite body frame are

$$\boldsymbol{L}_i^B = \begin{bmatrix} \cos(90-\gamma) & 0 & -\sin(90-\gamma) \\ 0 & 1 & 0 \\ \sin(90-\gamma) & 0 & \cos(90-\gamma) \end{bmatrix} \times \begin{bmatrix} \cos(\beta_i) & \sin(\beta_i) & 0 \\ -\sin(\beta_i) & \cos(\beta_i) & 0 \\ 0 & 0 & 1 \end{bmatrix} \begin{bmatrix} \cos(\alpha) & 0 & \sin(\alpha) \\ 0 & 1 & 0 \\ -\sin(\alpha) & 0 & \cos(\alpha) \end{bmatrix} \boldsymbol{L}_i^S \quad (1)$$

$$\boldsymbol{L}_o^B = \begin{bmatrix} \cos(90-\gamma) & 0 & -\sin(90-\gamma) \\ 0 & 1 & 0 \\ \sin(90-\gamma) & 0 & \cos(90-\gamma) \end{bmatrix} \times \begin{bmatrix} \cos(-\beta_o) & \sin(-\beta_o) & 0 \\ -\sin(-\beta_o) & \cos(-\beta_o) & 0 \\ 0 & 0 & 1 \end{bmatrix} \begin{bmatrix} \cos(\alpha) & 0 & \sin(\alpha) \\ 0 & 1 & 0 \\ -\sin(\alpha) & 0 & \cos(\alpha) \end{bmatrix} \boldsymbol{L}_o^S \quad (2)$$

where the crossing vectors in the sensor frame are both given as unit vectors in the Z^S direction. Then the horizon crossing vectors in the body frame are given as

$$\boldsymbol{L}_i^B = \begin{bmatrix} \cos(90-\gamma)\cos(\beta_i)\sin(\alpha) - \sin(90-\gamma)\cos(\alpha) \\ -\sin(\beta_i)\sin(\alpha) \\ \sin(90-\gamma)\cos(\beta_i)\sin(\alpha) + \cos(\alpha)\cos(90-\gamma) \end{bmatrix} \quad (3)$$

$$\boldsymbol{L}_o^B = \begin{bmatrix} \cos(90-\gamma)\cos(\beta_o)\sin(\alpha) - \sin(90-\gamma)\cos(\alpha) \\ \sin(\beta_o)\sin(\alpha) \\ \sin(90-\gamma)\cos(\beta_o)\sin(\alpha) + \cos(\alpha)\cos(90-\gamma) \end{bmatrix}$$

The horizon crossing vectors and nadir vector in the body frame, $\boldsymbol{N}^B$, satisfy the following:

$$\boldsymbol{L}_i^B \cdot \boldsymbol{N}^B = \cos(\eta); \qquad \boldsymbol{L}_o^B \cdot \boldsymbol{N}^B = \cos(\eta) \quad (4)$$

where η is the half-Earth disk angle and a function of Earth's equatorial radius r_e and satellite altitude h:

$$\eta = \sin^{-1}[r_e/(r_e + h)] \quad (5)$$

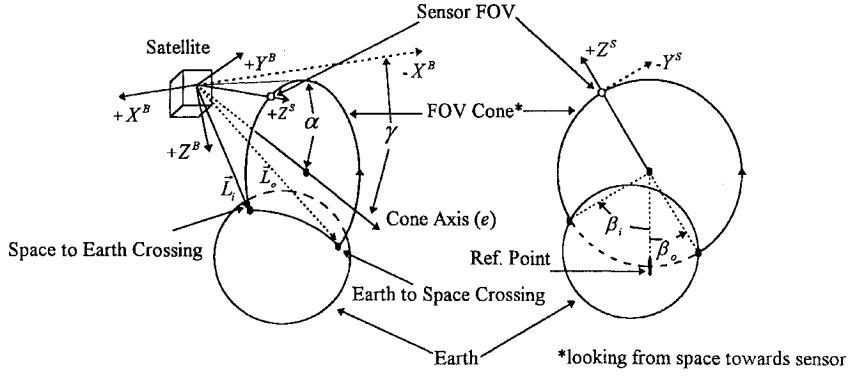

Fig. 1 Geometry of a scanning horizon sensor.

Received March 27, 1995; revision received Nov. 9, 1995; accepted for publication Dec. 14, 1995.
*Senior Member, Technical Staff, Control Analysis Department.
†Senior Member, Technical Staff, Electromechanical Control Department.
‡Engineer Specialist, Flight Software Validation Department.